Planar defects in three-dimensional chalcogenide glass photonic crystals

Elisa Nicoletti,[1] Douglas Bulla,[2] Barry Luther-Davies,[2] and Min Gu[1,*]

[1]*Centre for Micro-Photonics and Centre for Ultrahigh-Bandwidth Devices for Optical Systems, Faculty of Engineering and Industrial Sciences, Swinburne University of Technology, P.O. Box 218 Hawthorn, 3122 Victoria, Australia*

[2]*Laser Physics Centre and Centre for Ultrahigh-Bandwidth Devices for Optical Systems, Research School of Physical Sciences and Engineering, Australian National University, Canberra Australian Capital Territory 0200, Australia*

**Corresponding author: mgu@swin.edu.au*

Received April 15, 2011; revised May 14, 2011; accepted May 16, 2011; posted May 16, 2011 (Doc. ID 145890); published June 8, 2011

Here we report on the direct laser writing fabrication of Fabry–Perot-type planar microcavities in a three-dimensional (3D) photonic crystal (PhC) embedded within a high-refractive nonlinear chalcogenide glass (ChG) film. The fabricated planar microcavities in a nonlinear ChG 3D PhC facilitate the observation of resonant modes inside the stop gap. The experimental results show that the length of the planar cavity can be well controlled by the fabrication power and thus be used to tune the defect modes. The tunability of the observed defect modes is confirmed by the theoretical prediction.

OCIS codes: 220.4000, 230.5298, 230.4320.

Chalcogenide glasses (ChGs) have recently attracted much interest in the photonics community due to the excellent transparency in the mid-IR, the low phonon energies, and the high linear and nonlinear refractive indices [1–6]. In particular, photosensitive ChGs have recently been utilized as a unique building block for three-dimensional (3D) photonic crystals (PhCs) [3,5,7–10]. The periodic modulation of the refractive index allows for an effective control over light propagation and light–matter interactions, making PhCs an ideal platform for optical devices. The high nonlinearity of ChGs allows for a dynamical tunability of the PhCs properties and further advancement of all optical devices. While PhCs can confine and guide light at a submicrometer scale, the Kerr nonlinearity of the ChGs can be exploited to achieve compact integrated devices [9,11,12].

In order to provide the functionality to PhCs, the introduction of controlled defects is required. A large variety of optical microdevices are based on specific deviations from the ideal lattice periodicity. The introduction of defects creates allowed states for particular photon frequencies otherwise rejected by the surrounding photonic bandgap (PBG). The disruption of the periodicity can, in fact, provide a high degree of both spatial and temporal light confinement and custom design PhCs that allow precise control over the frequencies and directions of propagating electromagnetic waves. Although direct laser writing (DLW) based on a multiphoton-induced polymerization process has been successfully adopted to produce 3D nonlinear ChG PhCs [2,5], no defect has been produced within 3D functional stop gaps.

In this Letter, we present how planar Fabry–Perot-type defects can be introduced inside the 3D nonlinear ChG woodpile PhC using the DLW fabrication method. The cavity size was carefully chosen in order to satisfy the diffraction rules of a simple Fabry–Perot etalon. Resonant modes within the PBG were experimentally observed, as predicted by the theoretically analysis.

3D ChG PhCs were fabricated focusing femtosecond laser pulses (~200 fs) operating at wavelength 800 nm and a 1 KHz repetition rate inside a ~20 μm thick As_2S_3 film with an oil immersion objective (Olympus, NA 1.4, 100×) in an experimental setup reported elsewhere [5]. A schematic diagram of the 3D woodpile PhC produced by the multiphoton polymerization process [2,5] is illustrated in Fig. 1(a). Because of the limited NA of an objective used for focusing the laser beam, the polymerized rods are axially elongated [2,5].

We introduced microcavities at the center of a 16-layer woodpile PhC by simply modifying the computer-based design, as illustrated in Fig. 1(b). The woodpile structure provides a 3D mechanically stable design where the lattice parameters can be easily tuned as desired. After the eighth layer, a plane was fabricated by scanning multiple lines side by side with an offset of 50 nm between each other in the x direction. The minimum cavity length corresponds to the height of the axially elongated rods.

The thickness of the planar defect can be increased by scanning another layer of multiple lines with a small offset in the z direction.

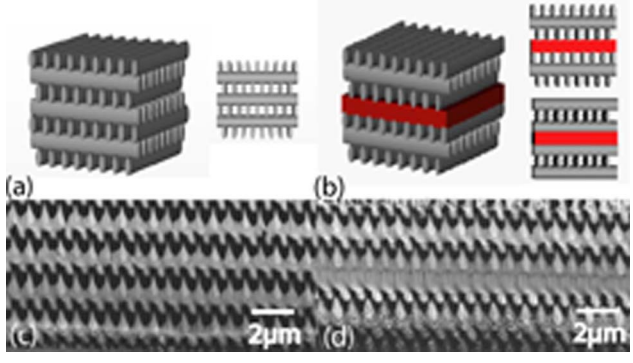

Fig. 1. (Color online) Sketches of the woodpile structure (a) without and (b) with the planar defects in the middle. SEM images (side views) of the fabricated woodpile ChG PhCs (c) without and (d) with the planar defects. Scale bar: 2 μm.

0146-9592/11/122248-03$15.00/0

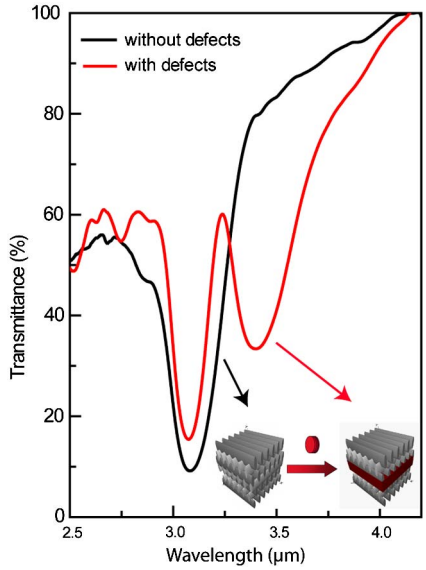

Fig. 2. (Color online) FTIR transmission spectra of the woodpile ChG PhC without defects (black curve) and after the introduction of a 1.5 μm thick planar defect. (inset) Sketch of the fabrication mechanism of a woodpile structure with a planar cavity of size d in the center.

The two portions of the PhC, each consisting of two eight-layer woodpile structures, act as the two parallel flat semitransparent mirrors of a conventional Fabry–Perot etalon [13]. As such, the constructive peaks of the Fabry–Perot cavity are given by

$$d = m\frac{\lambda}{2n \cdot \cos\theta}, \tag{1}$$

where d is the effective cavity length, m an integer, λ the light wavelength, n the cavity refractive index, and θ the angle of the incoming light beam. Since the elongated shape of the woodpile rods in the z direction limits the minimum length of the cavity, we expect to observe only the second-order constructive interference peak.

Side view scanning electron microscope (SEM) images of a PhC without and with the plane defect are presented in Figs. 1(c) and 1(d). The lattice spacing dx and the layer spacing dz are 1 μm and 0.96 μm, respectively. Fourier transform IR (FTIR) measurements of such structures were performed using a Nicolet Nexus FTIR spectrometer with a Continuum IR microscope (Thermo Nicolet, Madison, Wisconsin, USA) and reported in Fig. 2. The black curve refers to the 16-layer PhC without defects, which presents a dip in the transmission spectrum centered at wavelength 3.1 μm. The red curve represents the transmission spectra of the PhC with the same lattice parameters, but with a plane defect, 1.5 μm thick, between the eighth and the ninth layers. A sharp peak within the stop gap region is observed for a cavity length of 1.5 μm corresponding to the second order of constructive interference conditions [see Eq. (1)].

In order to shift the PBG and hence the defect mode to telecommunication wavelength, it is necessary to reduce the PhC feature size. The issue of the axial elongation of the rods could be addressed with the implementation of a shaded-ring filter centered in the objective aperture stop. The aspect ratio could be in this way reduced by about

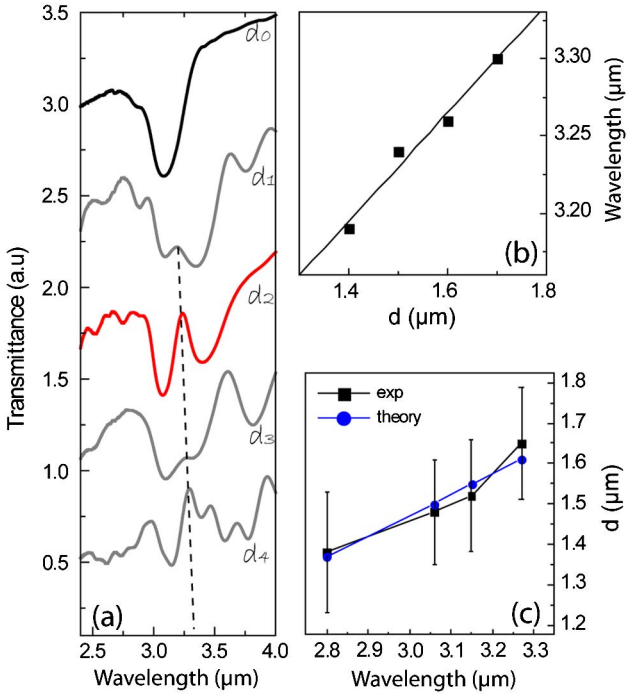

Fig. 3. (Color online) (a) FTIR transmission spectra of ChG PhCs for different microcavity lengths ($d_1 = 1.38\,\mu$m, $d_2 = 1.48\,\mu$m, $d_3 = 1.58\,\mu$m, $d_4 = 1.68\,\mu$m). d_0 corresponds to the spectrum of the reference ChG PhC without defect. (b) Experimental plot of the cavity length (d) versus the position of the cavity mode confirming a linear dependence. (c) Experimental (squares) and theoretical (circles) plots of the mode peak position versus the cavity size at which it occurs for different fabrication conditions, as reported in Table 1.

20% [14,15]. Furthermore, by changing the laser beam repetition rate, it could be possible to exploit the accumulation of heating at the focal spot and push the threshold rod size to less then 100 nm [16].

Additional improvements in the fabrication condition could be achieved by the compensation for the strong spherical aberration during DLW in high refractive index material [17]. The implementation of an adaptive optics system into a laser microfabrication setup could lead to enormous improvements to the fabrication conditions and reduce the elongation of the polymerized rods by a factor of 4 even at a depth of about 20 μm. The reduced aspect ratio may allow for a reduction of the interlayer spacing (dz) and lead to PhCs with functionality at wavelengths lower than 1.5 μm.

A series of PhC planar microcavities were fabricated with d ranging from 1.38 to 1.68 μm, as well as a reference structure without a defect. Both the PhC lattice parameters ($dx = 1\,\mu$m and $dz = 0.96\,\mu$m) and the laser beam power (4 μW) were maintained constant. The minimum cavity length (d_1) is determined by the dimensions of

Table 1. Cavity Length for Different Fabrication Powers

$P(\mu W)$	$d_1(\mu m)$	$d_2(\mu m)$	$d_3(\mu m)$	$d_4(\mu m)$
3	1.08	1.18	1.28	**1.38**
3.5	1.38	**1.48**	1.58	1.68
4	1.42	**1.52**	1.62	1.72
4.5	1.45	1.65	**1.65**	1.75

the rods under the given power used for the fabrication. We increased the length of the microcavity, scanning another layer of multiple lines at an offset in the z direction of $0.1\,\mu$m (d_2), $0.2\,\mu$m (d_3), and $0.3\,\mu$m (d_4). The FTIR transmission measurements are presented in Fig. 3(a). For all the cavity lengths, it was possible to observe a peak within the stop gap region that becomes more intense for a cavity length of $1.5\,\mu$m. In accordance with previous studies [18], the cavity mode shifts to the longer wavelength gap edge as the cavity size increases. A plot of the cavity length (d) versus the position of the cavity mode peak is presented in Fig. 3(b).

In order to confirm the theoretical prediction, further investigations were conducted by changing the filling ratio of the PhCs hosting the microcavities. A series of PhCs were fabricated with the same lattice parameters ($dx = 1\,\mu$m, $dz = 0.96\,\mu$m) but at different laser powers.

The variation of the laser power affects the rod dimensions, i.e., the bandgap positions and the cavity sizes. Once again we fabricated microcavites of different length inside the PhCs and measured the FTIR transmission spectra. The experimental values for the cavity length according to the laser power are illustrated in Fig. 3(c) and summarized in Table 1.

The highlighted numbers refer to the cavity size for which we observed the maximum peak mode in the FTIR transmission spectra. Taking into account the redshift of the bandgap position with the increasing of the laser power [5], it is possible to predict the cavity length that satisfies the constructive interference rules in Eq. (1).

Figure 3(c) shows a plot of the experimental and calculated values for the mode peak position versus the cavity size at which it occurs. The experimental values are in good agreement with the predictions given by Eq. (1).

In conclusion, we have demonstrated the introduction of defects in 3D periodic structures within photosensitive nonlinear ChGs by DLW through a multiphoton polymerization process. Fabry–Perot-type cavities have been fabricated and engineered inside a 3D ChG PhC. The FTIR transmission spectra show the presence of resonant modes inside the stop gap, which depends on the cavity length. The introduction of designed defects and the tunability of the cavity modes in the 3D nonlinear PhCs are crucial for the realization of functional photonic devices and switches toward optical integrated circuits.

This work was produced with the assistance of the Australian Research Council (ARC) under its Centers of Excellence program. The Centre for Ultrahigh-Bandwidth Devices for Optical Systems (CUDOS) is an ARC Centre of Excellence.

References

1. S. J. Madden, D. Y. Choi, M. R. E. Lamont, V. G. Ta'eed, N. J. Baker, M. D. Pelusi, B. Luther-Davies, and B. J. Eggleton, Opt. Photon. News **19** (2), 18 (2008).
2. K. Paivasaari, V. K. Tikhomirov, and J. Turunen, Opt. Express **15**, 2336 (2007).
3. S. Wong, M. Deubel, F. Pérez-Willard, S. John, G. A. Ozin, M. Wegener, and G. Von Freymann, Adv. Mater. **18**, 265 (2006).
4. M. Galili, J. Xu, H. C. H. Mulvad, L. K. Oxenløwe, A. T. Clausen, P. Jeppesen, B. Luther-Davis, S. Madden, A. Rode, D. Y. Choi, M. Pelusi, F. Luan, and B. J. Eggleton, Opt. Express **17**, 2182 (2009).
5. E. Nicoletti, G. Zhou, B. Jia, M. J. Ventura, D. Bulla, B. Luther-Davies, and M. Gu, Opt. Lett. **33**, 2311 (2008).
6. V. G. Ta'eed, N. J. Baker, L. Fu, K. Finsterbusch, M. R. E. Lamont, D. J. Moss, H. C. Nguyen, B. J. Eggleton, D. Y. Choi, S. Madden, and B. Luther-Davies, Opt. Express **15**, 9205 (2007).
7. A. Feigel, Z. Kotler, B. Sfez, A. Arsh, M. Klebanov, and V. Lyubin, Appl. Phys. Lett. **77**, 3221 (2000).
8. A. Feigel, M. Veinger, B. Sfez, A. Arsh, M. Klebanov, and V. Lyubin, Appl. Phys. Lett. **83**, 4480 (2003).
9. D. Freeman, C. Grillet, M. W. Lee, C. L. C. Smith, Y. Ruan, A. Rode, M. Krolikowska, S. Tomljenovic-Hanic, C. M. de Sterke, M. J. Steel, B. Luther-Davies, S. Madden, D. J. Moss, Y. H. Lee, and B. J. Eggleton, Photon. Nanostr. Fundam. Appl. **6**, 3 (2008).
10. D. Freeman, S. Madden, and B. Luther-Davies, Opt. Express **13**, 3079 (2005).
11. C. Monat, C. Grillet, P. Domachuk, C. Smith, E. Magi, D. J. Moss, H. C. Nguyen, S. Tomljenovic-Hanic, M. Cronin-Golomb, B. J. Eggleton, D. Freeman, S. Madden, B. Luther-Davies, S. Mutzenich, G. Rosengarten, and A. Mitchell, Laser Phys. Lett. **4**, 177 (2007).
12. Y. Ruan, M. K. Kim, Y. H. Lee, B. Luther-Davies, and A. Rode, Appl. Phys. Lett. **90**, 071102 (2007).
13. F. L. Pedrotti and L. S. Pedrotti, *Introduction to Optics*, 2nd ed. (Prentice-Hall, 1993).
14. C. Ibáñez-López, G. Saavedra, G. Boyer, and M. Martinez-Corral, Opt. Express **13**, 6168 (2005).
15. M. Martinez-Corral, C. Ibáñez-López, G. Saavedra, and M. Caballero, Opt. Express **11**, 1740 (2003).
16. A. H. Nejadmalayeri and P. R. Herman, Opt. Express **15**, 10842 (2007).
17. B. P. Cumming, A. Jesacher, M. J. Booth, T. Wilson, and M. Gu, Opt. Express **19**, 9419 (2011).
18. M. J. Ventura, M. Straub, and M. Gu, Opt. Express **13**, 2767 (2005).